2.5 Bit/Detected Photon Demonstration Program: Phase II and III Experimental Results

J. Katz
Communications Systems Research Section

This report describes recent progress in the experimental program for demonstrating, in the lab, an energy-efficient optical communication channel operating at a rate of 2.5 bits/detected photon. Results of the uncoded PPM channel performance are presented. These results indicate that the above throughput efficiency can be achieved not only with a Reed-Solomon (255, 191) code as originally predicted, but with less complex (255, 223) code as well.

I. Introduction

The purpose of this report is to describe the progress in the experimental program by demonstrating in the lab an energy-efficient optical communication channel operating at a rate of 2.5 bits/detected photon. The overall scope and analysis of the program, including phase-I experimental results, were described in an earlier report (Ref. 1), and the more general aspects and advantages of free space optical communications can be found in Refs. 2 and 3.

For the sake of completeness, the block diagram of the demonstration system (Ref. 1) is shown in Fig. 1. The optical portion of the system consists mainly of a gallium arsenide semiconductor injection laser and a direct detection photomultiplier tube. Surrounding the optoelectronic components are the modulation and coding hardware, namely, a 256 slot/word PPM modulation/demodulation system and an 8-bit Reed-Solomon encoding/decoding system, respectively. The demonstration program is divided into four phases, as indicated in Fig. 1. Phase I (Ref. 1) involved only the PMT and its associated preamplifier and was concerned with characterizing the dark current noise distribution of the detection system. This report describes phase II (measuring optical pulse erasure and error statistics) and phase III (measuring PPM word error and word erasure probabilities). The final phase (not described here) will encompass the coding hardware and will demonstrate the 2.5 bits/detected photon goal.

The outline of this report is as follows. In Section II the calibration of the optical link is described. Correct calibration is essential for a relevant comparison between theory and experiment and a meaningful evaluation of the channel performance. Section III is concerned with the pulse detection statistics of the photomultiplier tube (PMT). Finally, Section IV presents the results of the uncoded PPM link. The modulation scheme used is 256 slots/word PPM, transmitted at a rate of 39,062 words/sec, which corresponds to an uncoded data rate of 312 kbits/sec. This rate is more than twice the benchmark rate of Voyager at Jupiter. Projecting from the experimental results of the uncoded PPM into the coded performance, we can predict with greater confidence that the energy efficiency goal of 2.5 bits/detected photon can be achieved.

II. Calibration of Optical Link

The calibration of the optical link is a crucial step in the experiment, since in order to determine the absolute performance of the system in terms of bits/detected photon, the number of detected photons must be determined as accurately as possible.

The optical setup inside the darkroom enclosure is shown in Fig. 2. The light emitter is a GaAs injection laser diode (Mitsubishi, TJS type; model ML-3001). It emits light in a single spatial and longitudinal mode. The lasing wavelength of the laser diode used in this experiment was around 0.81 μm. The current flowing through the laser (i_L) is monitored with a current probe (American Laser Systems, model 711), and the power emitted out of the laser (P_L) is monitored by a photodiode which is included in the laser package (not shown in Fig. 2). These two parameters $(i_L$ and $P_L)$ are not important for this particular experiment, but they have to be monitored so as to not exceed the absolute maximum range ratings of the device. The light emitted by the laser is collimated by a lens and passed through an iris diaphragm which limits the spatial extent of the beam to dimensions smaller than those of the photomultiplier tube (PMT) photocathode. A cube beam-splitter diverts part of the laser radiation into a calibrated photodiode (UDT, model PIN-10), which monitors the actual amount of light entering the photomultiplier tube. The other portion of the light is attenuated by neutral density filters (and, to some extent, also by other glass surfaces which are present in front of the photocathode, e.g., PMT faceplate, PMT housing window). The signal of the calibrated photodiode is amplified and displayed on an oscilloscope. The output signal of the PMT is amplified and fed into a counter (HP5370A). By a straightforward calculation one can find that the number of photoelectrons counted per second N_{pe} is related to the photodiode voltage signal displayed on the oscilloscope V_{pd} by the following formula

$$N_{pe} = \frac{\eta\lambda\left(\frac{T}{R}\right)}{ZA\sigma hcL} (DF)P_d V_{pd} \tag{1}$$

where η is the quantum efficiency of the PMT's photocathode, λ is the radiation wavelength, (T/R) is the ratio between the intensity of the wave transmitted by the beamsplitter to the intensity of the wave reflected by it, Z is the impedance seen by the photodiode, A is the amount of amplification of the photodiode signal, σ is the responsivity of the photodiode, h is Planck's constant, c is the vacuum light velocity, L is the total amount of attenuation (i.e., the ratio between the power transmitted by the beamsplitter and the power incident on the PMT photocathode), DF is the duty factor of the light signal, and P_d is the probability of counting a photoelectron once it

is released by the photocathode. In our case $\lambda = 0.81$ μm, $(T/R) = 32/68$, $Z = 50\Omega$, $A = 100$, $\sigma = 0.3$ A/W, and $\eta = 0.16$. Using these parameters, Eq. (1) reduces to

$$N_{pe} = 2.05 \cdot 10^{14} \frac{(DF)P_d}{L} V_{pd} \tag{2}$$

The attenuations of the individual filters were measured and calibrated separately. The overall attenuation – which was typically of the order of 50 to 70 dB – was obtained by using a stack of filters. Several sets of filters of different makes and types (both absorption and reflection) were used in order to assure that the results do not depend on a particular set where interference-type interactions between the elements might change the overall attenuation. All the calibrators of the beam-splitter and filters were done at the actual laser wavelength. Also, in order to prevent errors due to undetected problems in certain devices, the measurements were repeated for two photomultiplier tubes, two laser diodes, and the calibrated photodiode response was compared to that of another calibrated photodiode. Finally, in order to virtually eliminate the effect of P_d, the system operated in the region where $P_d \sim 1$. This corresponds to the experimental condition of setting the gain of the PMT as high as possible ($\leqslant 10^7$), while, at the same time, reducing the counter threshold as much as possible but still without having significant contribution of thermal-Gaussian noise.

Before concluding this section we want to comment on the strength of the optical signal used. In order to make intrinsic noise contributions insignificant and to increase the quality of the average estimates, the number of signal photons was made much larger than the number of dark counts. The upper limit on the signal strength was set by PMT reliability considerations (the absolute maximum rating is about $6 \cdot 10^5$ photoelectrons/second) and by the need to minimize the probability that two detection events partly or totally overlap so they are counted as one event. Typical values were around $10^4 - 5 \cdot 10^4$ photoelectrons/second.

The experimental calibration measurements were in accordance with the calculated results. The experimental error is about 10 - 15%, and is due mainly to inaccuracies of the measurements of the optical attenuation and the estimate on the quantum efficiency, especially due to its dependence on temperature.

III. Single Pulse Detection Statistics

This section describes the experiment of measuring the probability P_{ds} of correctly detecting the presence of incident laser light during a time slot. The basic experimental setup is

shown in Fig. 3. The laser driver is a HP8003A pulse generator. The optical system is the same as that shown in Fig. 2. The photomultiplier tube is an RCA model C31034A, which has a GaAs photocathode and is the best commercially available PMT for the 0.85-μm region of the spectrum. The preamplifier is an ORTEC model 9301 (gain ≈ 10, beandwidth ≈ 150 MHz), and the final amplifier is one specifically designed and built around a μA733 video amplifier. It can operate in different gains and bandwidths, but the nominal values used in the experiment were a gain of 80 and a bandwidth of 80 MHz. Its RMS input noise over a 100-MHz bandwidth is 30 μV, and although it has a smaller bandwidth than the HP461 amplifier used in phase 1 of the experiment (Ref. 1), its overall performance is better because of its higher dynamic range and better saturation characteristics. In some experiments we also used a Comlinear model CLC-102 video amplifier, which has a 250-MHz bandwidth, and the results obtained were similar. The delay unit used was a HP8013A pulse generator. It is needed to synchronize the time-slot clock with the received light pulse. The computing controller used for averaging the counts over long periods was a HP9845C. The detector unit used was one specifically designed and built for this experiment. In Ref. 1 the performance of a detector which is based on an integrate-and-dump procedure was suggested and analyzed. Because of two reasons we did not employ this detector structure in our experiment. First, it is difficult to realize integrate-and-dump circuitry at the needed speeds. Secondly, and more important, the integrate-and-dump scheme is not the optimum detection method, since typically the signal is present only over a small fraction of the time slot, while the noise is integrated over the entire slot. The actual detector circuit used in our experiment employed hard-decision in each time-slot, and it produced reasonable results. The subject of the optimum detection scheme for this type of received signal is still an open issue and is under investigation.

In the experiment the laser diode was pulsed in a duty cycle of 1/256, with pulses of 100-nS duration (i.e., 39,062 pulses per second). Figure 4 shows several examples of the amplified PMT output under illumination intensity level corresponding to approximately one photoelectron per 100-nS time slot. The different signals occurring in each case are due to the fact that they are sample functions of the generating Poisson process. The experimental value of P_{ds} was determined by dividing the average number of time slots per second where a signal was detected by 39,062

In Fig. 5, the probability P_{ds} of detecting the incident light is shown as a function of the average intensity of light measured in detected photons (i.e., photoelectrons) per slot. The parameter on the curves in this figure is the PMT gain. The threshold value of the detector was set at 80 mV, which is just above the value where thermal noise becomes significant. We see that for

N_s = 3.2 detected photons/slot, which corresponds to 2.5 bits/ detected photon when using 8-bit PPM, we can obtain detection probabilities P_{ds} exceeding 90%. The experimental results are upper bounded by

$$P_{ds} \leq 1 - e^{-N_s} \qquad (3)$$

which is the result for the ideal counter.

Figure 5 should be compared with the receiver operating curves of Ref. 1. Since an erroneous noise variance was used in Ref. 1, we are using for comparison the corrected results of Ref. 4. In particular, Fig. 7 of Ref. 4, combined with our experimental results from Fig. 5, is shown in Fig. 6. It is interesting to note that the experimental results – using the hard decision detector – are very similar to the theoretical results – using the integrate-and-dump scheme. The subject of the theoretical analysis of the hard decision detector is under current investigation.

IV. Uncoded PPM Performance

This part of the experiment constitutes the third phase of the experimental program. The experimental setup is shown in Fig. 7. The synthesizer used as the master clock is a SYNTEST model SI-102. The frequency was 39,062 Hz, which corresponds to 100-ns time slots in a 256-slots/word PPM configuration. The PPM modulator/demodulator is an instrument designed and built specifically for the 2.5-bits/detected photon program, and its functions and performance are the subject of a separate report (Ref. 5). Since it contains almost all the necessary performance diagnostics, no additional equipment (except for the "AND" gate) was needed for the error rate measurements. These diagnostics include indications of PPM word errors as well as indications of the number of slots detected during each word period (i.e., 0 (erasure), 1 (single), 2 (double) or >2 (overflow)). The "AND" gate is needed in order to synchronize these indications with the demodulator "strobe" output. The remainder of the equipment used in this setup was described in the last two sections.

In the experiment the laser diode was pulsed (1/256 duty-factor; 100-ns slot time), and the number of the various events (errors, erasures, etc.) was counted. We found that in our case we are limited by erasures, which outnumber errors by more than one order of magnitude. The validity of this condition needs to be checked in any new situation (e.g., space-based receivers), since the performance of the Reed-Solomon decoder degrades when the ratio of erasures to errors decreases. It should be noted that only the information was transmitted optically, the synchronization signals were hard-wired between the modulator and the demodulator.

The results of the measurements are shown in Fig. 8, which depicts the bit error probability P_b as a function of the average number of detected photons per slot N_s, with the PMT gain as a parameter. Also shown on the graph is the lower bound

$$P_b = \frac{256}{510} e^{-N_s} \sim \frac{1}{2} e^{-N_s} \qquad (4)$$

which is the expression of the ideal photon counter. We see that the experiment results are not too far from this bound.

Figure 9 compares the three results, i.e., the ideal photon counter, experimental results, and the integrate-and-dump detector theoretical results from Ref. 1 (but with the correct noise variance), under two PMT gains: 10^6 and $3 \cdot 10^6$. For $G = 10^6$ (Fig. 9a), the experimental hard-decision results are somewhat better than the theoretical integrate-and-dump result. As we increase the gain ($G = 3 \cdot 10^6$, Fig. 9b), both results move closer to the ideal counter, with the (theoretical) integrate-and-dump results somewhat better than the (experimental) hard-decision results.

In order to predict the coded channel performance on the basis of our measurements, we need the relation between the coded and uncoded performance. This relation is shown in Fig. 10. The various curves associated with a given code correspond to different combinations of errors and erasures.

Comparing the results of Figs. 8 and 10, we see that the needed energy efficiency of 2.5 bits/detected photon can be easily achieved with the rate 3/4 code at the desired bit error probability of $5 \cdot 10^{-3}$. From these graphs it also seems that if the ratio of erasures to errors is not too low, operation at 2.5 bits/detected photon can be achieved even with the rate 7/8 code which has less complexity.

V. Conclusions

The uncoded performance of a laboratory optical channel has been demonstrated and evaluated. The results agree with the previously generated theoretical analysis, thus substantially increasing the confidence that the energy-efficient operation of 2.5 bits/detected photon will be achieved using a rate 3/4 Reed-Solomon code, as well as possibly with a less complex rate 7/8 code.

Acknowledgment

References

1. Lesh, J. R., Katz, J., Tan, H. H., and Zwillinger, D., "2.5 Bits/Detected Photon Demonstration Program Description, Analysis, and Phase I Results," *TDA Progress Report 42-66*, pp. 115-132, Jet Propulsion Laboratory, Pasadena, Calif., Dec. 15, 1981

2. Pierce, J. R., "Optical Channels: Practical Limits with Photon Counting," *IEEE Trans. Commun.*, COM-26, No. 12, pp. 1819-1821, Dec. 1978.

3. Katz, J., "High Power Semiconductor Lasers for Deep Space Communications," *TDA Progress Report 42-63*, pp. 40-50, Jet Propulsion Laboratory, Pasadena, Calif., June 15, 1981

4. Tan, H. H., "A Statistical Model of the Photomultiplier Gain Process with Applications to Optical Pulse Detection," *TDA Progress Report 42-68*, pp. 55-67, Jet Propulsion Laboratory, Pasadena, Calif., April 15, 1982

5. Marshall, W. K., "A PPM Modulator and Demodulator for the 2.5 Bit/Detected Photon Demonstration," *TDA Progress Report 42-68*, pp. 50-54, Jet Propulsion Laboratory, Pasadena, Calif., April 15, 1982
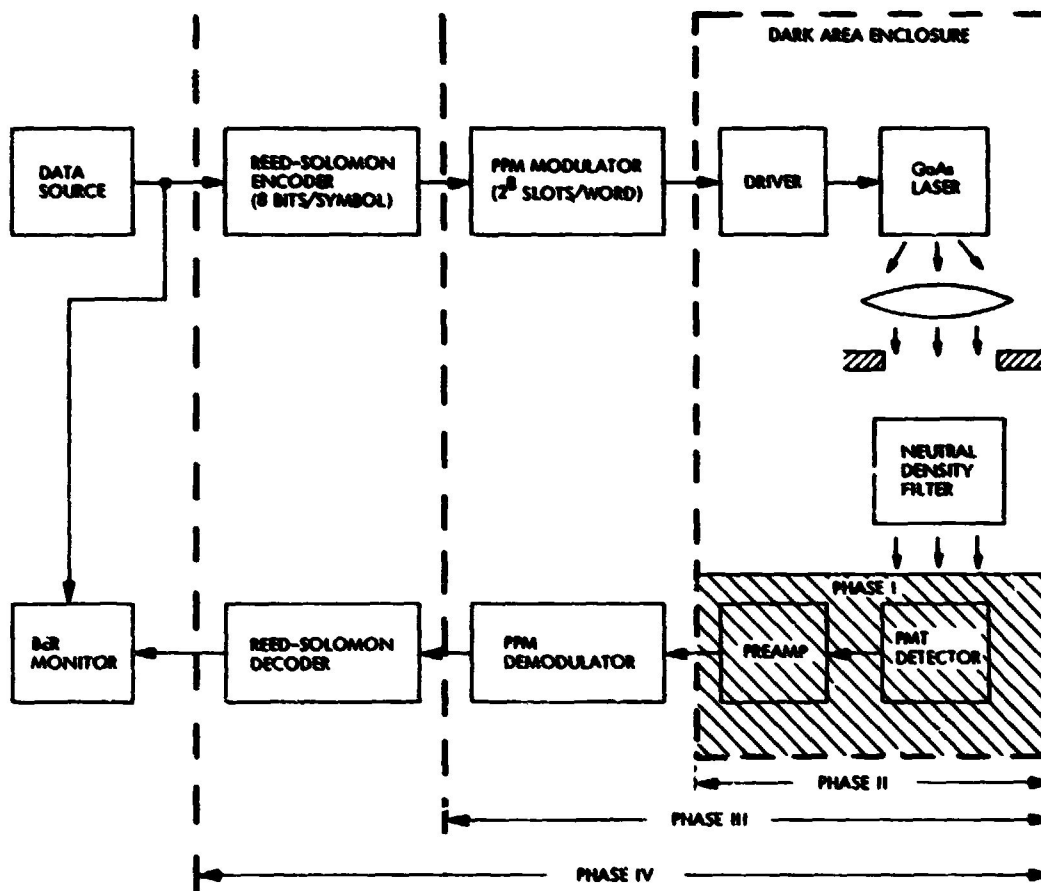
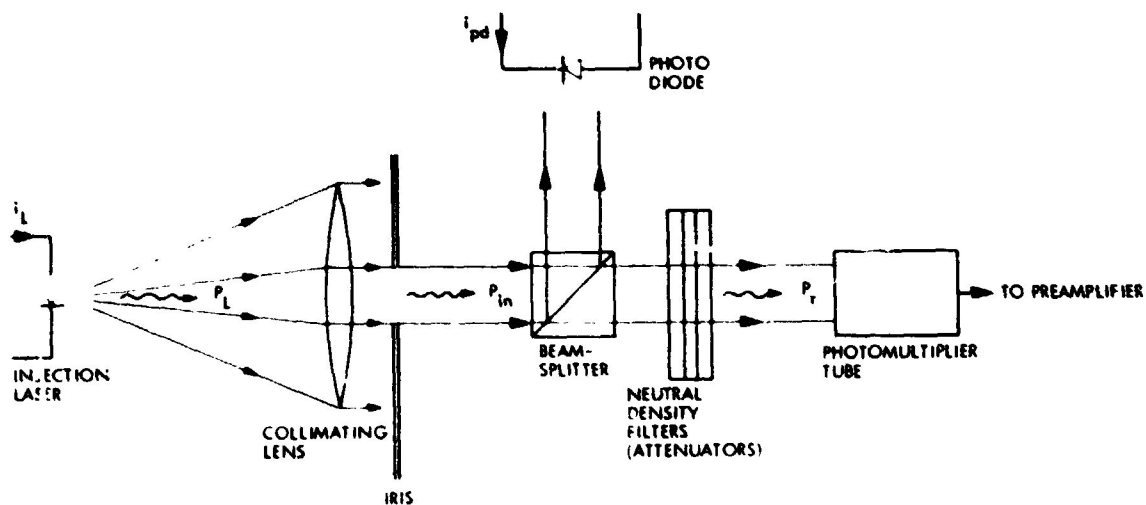Fig. 1. Block diagram of 2.5 bit/detected photon demonstration system with the various experimental phases

Fig. 2. Schematic view of the electrooptical components in the experiment
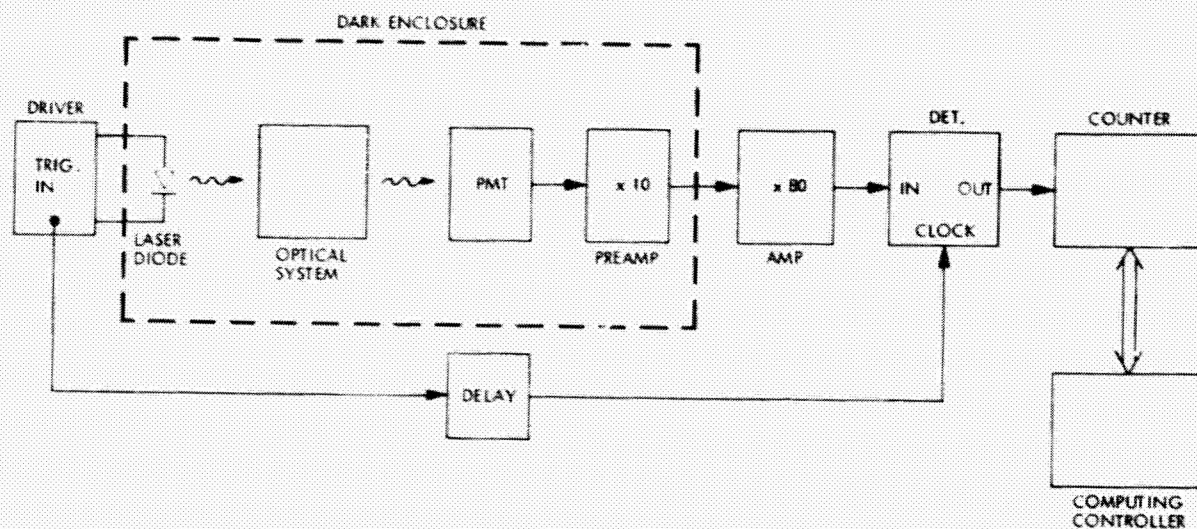
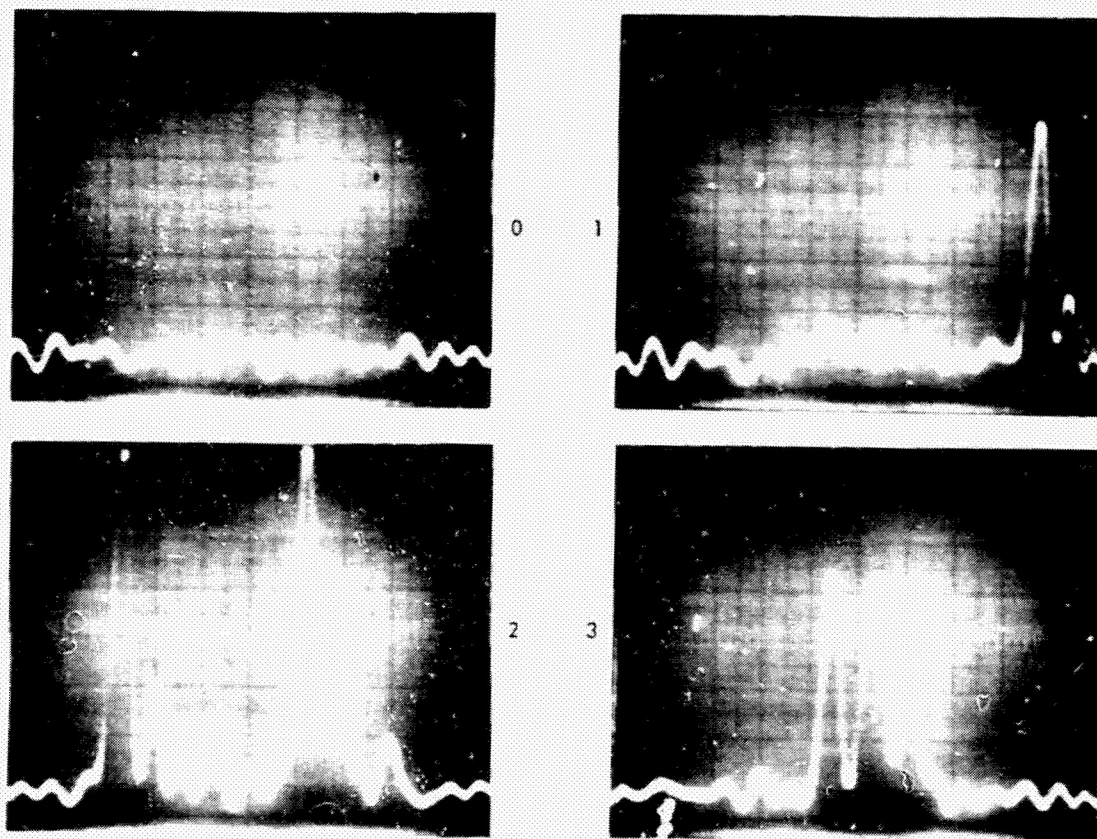Fig. 3. Block diagram of experimental setup for measurement of optical pulse detection probability P_{ds}

Fig. 4. Examples of various amplified PMT output oscilloscope traces during incidence of a light pulse with $\bar{N}_s = 1$ detected photon/slot (time slot is 100 ns). Shown are traces with 0, 1, 2 and 3 photoelectron events

Fig. 5. Measured optical pulse detection probability P_{ds} as a function of $\bar{N}_s$ (average number of photoelectrons per pulse) for several values of PMT gain. Also shown is the ideal upper bound $P_{ds} = 1-e^{-\bar{N}_s}$

Fig. 6. Binary communication receiver operating curve as a function of $\bar{N}_s$: comparison between theory and experiment
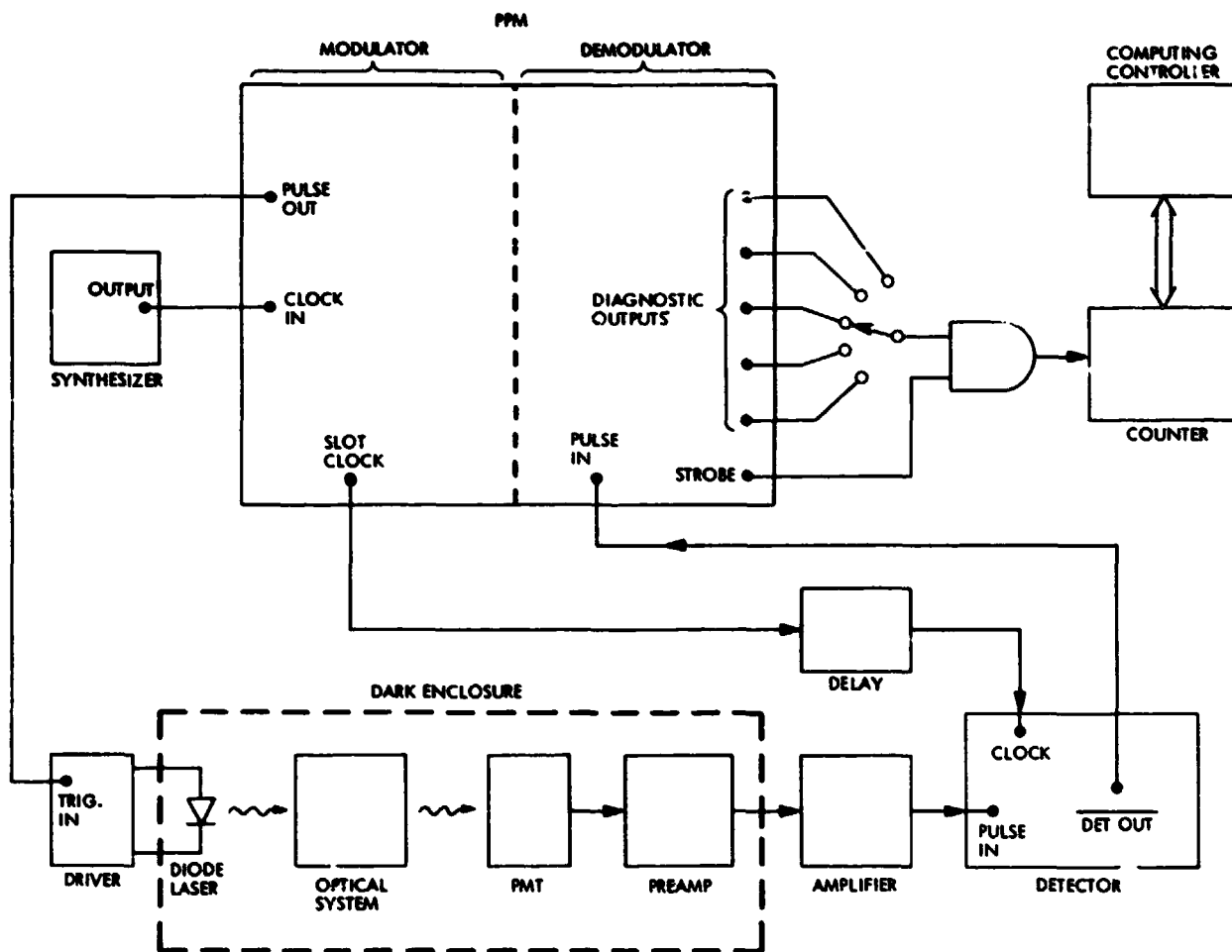
Fig. 7. Block diagram of experimental setup for measuring the uncoded, PPM-modulated error performance of the optical channel
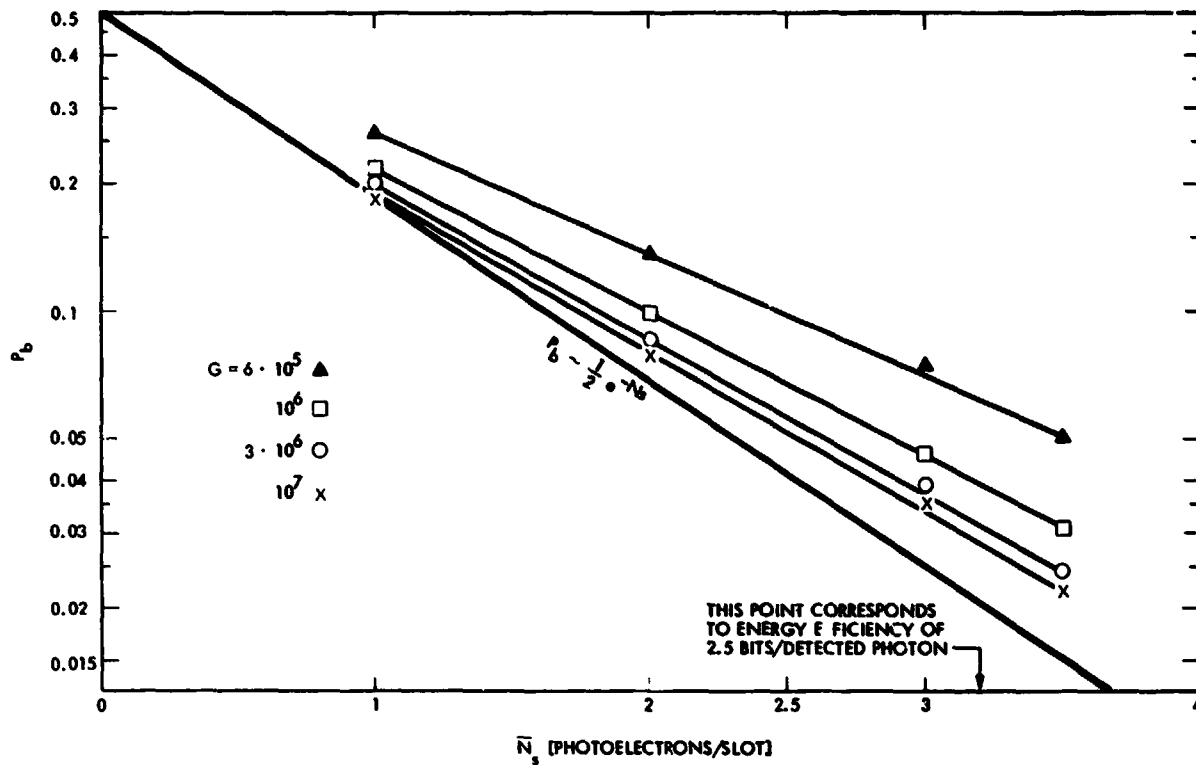
Fig. 8. Measured bit error performance for uncoded 256-ary PPM as a function of $\bar{N}_s$, the average number of detected photons/slot, for several values of PMT gain. $\bar{N}_s = 3.2$ corresponds to operation with energy efficiency of 2.5 bits/detected photon
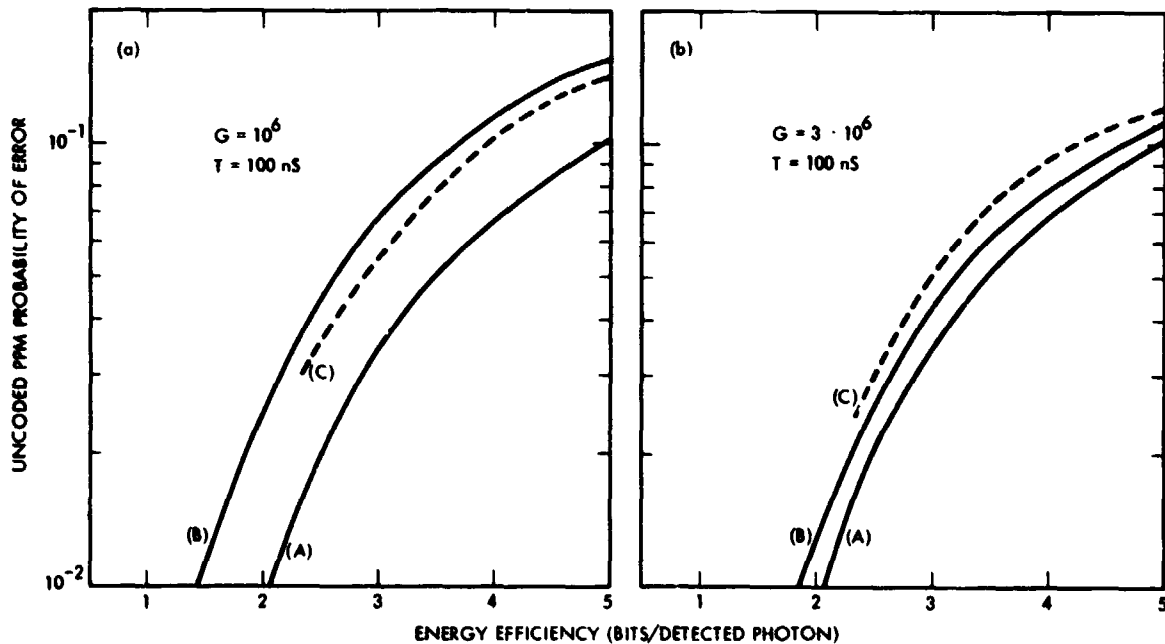

Fig. 9. Uncoded PPM bit error probability vs energy throughput efficiency (in bits/detected photon) for (a) PMT gain $= 10^6$ and (b) PMT gain $= 3.3 \cdot 10^6$. In every graph, (A) indicates the ideal counter, (B) the integrate-and-dump theoretical performance, and (C) the experimental results using hard decision, as taken from Fig. 8
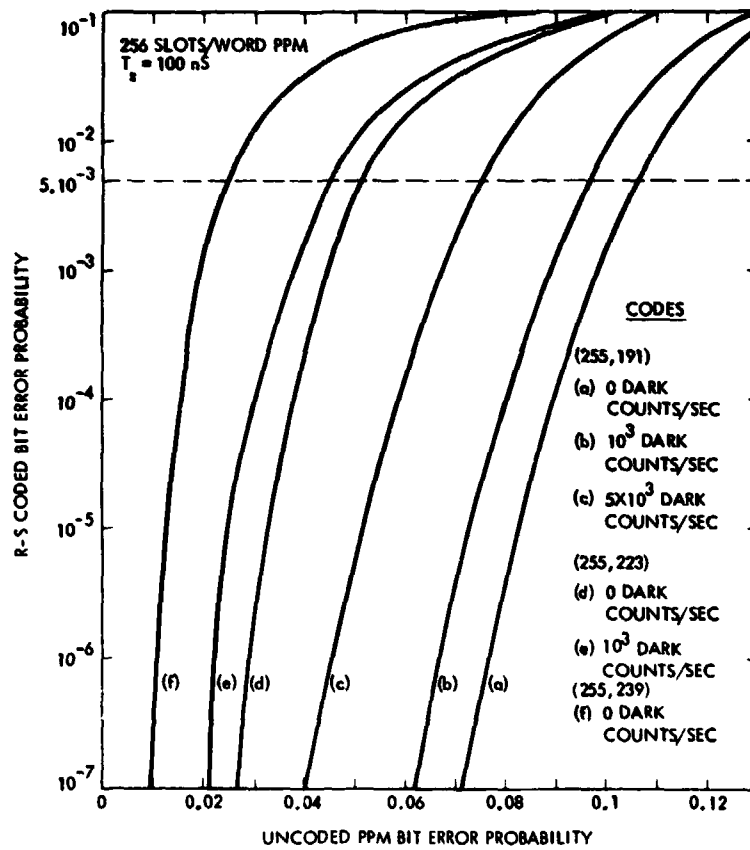
Fig. 10. RS coded bit error rate as a function of the uncoded PPM bit error rate for (255, 223) and (255, 191) codes and for the extreme combinations of errors and erasures